A theoretical model for local buckling of FRP-confined CFST columns

Yue-Ling Long [a,*], Xiang-Hua Yue [a], Sheng Ge [a], Leroy Gardner [b,*], M. Ahmer Wadee [b]

a. Department of Civil Engineering, Guangdong University of Technology, Guangzhou 510006, China.

b. Department of Civil and Environmental Engineering, Imperial College London, London SW7 2AZ, UK

*Corresponding authors: Yue-Ling Long(longyl@gdut.edu.cn) and Leroy Gardner (leroy.gardner@imperial.ac.uk)

Abstract: A theoretical model for the local buckling of FRP-confined concrete-filled steel tubular (CFST) columns under axial compression is proposed. The formulae for the elastic local critical buckling stress of the steel tube in FRP-confined CFST columns are derived using energy methods. Subsequently, a finite element (FE) model for local buckling of FRP-confined CFST columns is developed in order to verify the proposed model. The proposed model is calibrated with results from the FE model and tests, which exhibits good agreement. The proposed model is subsequently employed to investigate local buckling behaviour of the steel tube in FRP-confined CFST columns. It is found that the local critical buckling stress of the steel tube in FRP-confined CFST columns is significantly influenced by both the tensile stiffness ratios of FRP jackets to the steel tube, and the diameter-to-thickness ratios of the steel tube. The local critical buckling stress of the steel tube decreases with increasing diameter-to-thickness ratios of the steel tube, whereas the local critical buckling stress of the steel tube increases with the increase of the tensile stiffness ratios of FRP jackets to the steel tube at a specified value of diameter-to-thickness ratio. Furthermore, limitations on the diameter-to-thickness ratios of the steel tube in FRP-confined CFST columns are suggested for structural engineering practice. Finally, a novel concept, an equivalent thickness of the steel tube contributed by the FRP jackets, is proposed, resulting in a unified equation for the critical buckling stress of steel tubes in both FRP-confined CFST columns and conventional CFST columns.

Key words: Local buckling; Concrete-filled steel tube (CFST); Fibre reinforced polymer (FRP); Critical buckling stress;

1. Introduction

Concrete-filled steel tubular (CFST) columns are being extensively used in buildings, bridges and other structures owing to their high strength, high stiffness, good ductility and large energy absorption capacity. In the past few decades, a large number of experimental and analytical studies have been conducted to investigate the behaviour of CFST columns including those by Furlong [1-2], Ge et al. [3-4], Uy et al. [5-6], Sakino et al. [7], Zuo et al. [8-9], Abed et al. [10-11], Lai et al. [12] and Long et al. [13-14]. According these studies, the inward local buckling of the steel tube in CFST columns can be prevented by the concrete core. However, the outward local buckling of the steel tube in CFST columns can result in the degration in steel confinement, strength and ductility [15-17]. Against this background, Xiao proposed a novel form of CFST columns (i.e. FRP-confined CFST columns) to enhance the structural performance of CFST columns by using fibre reinforced polymers (FRP) to delay the occurrence of local buckling of the steel tube (Fig. 1). Following the initial work of Xiao [18], a large number of experimental and analytical studies have been conducted to investigate the behavior of FRP-confined CFST columns including those by Xiao et al. [19-21], Tao et al. [22], Teng et al. [15-17, 23-24], Prabhu et al. [25-26], Dong et al. [27], Alam et al. [28] and Shen et al. [29]. The results of these studies demonstrate that the FRP jackets can effectively delay or even prevent the outward local buckling of the steel tube of CFST columns, resulting in significantly improved structural performance subjected to either static loads or seismic loads.

However, the local buckling behaviour of the steel tube in FRP-confined CFST columns remains an open problem. To the best knowledge of the authors, no existing studies are available in the literature concerning the local buckling behaviour of the steel tube in FRP-confined CFST columns. To advance the understanding of the local buckling behavior of FRP-confined CFST columns, a theoretical model for the local buckling of FRP-confined CFST columns under axial compression is proposed currently. The model is verified against experimental results and is subsequently employed to investigate the influence of FRP jackets on the local critical buckling stress of steel tubes in FRP-confined CFST columns. Reasonable ranges for the diameter-to-thickness ratios of the steel tube in FRP-confined CFST columns are suggested and a unified equation for the local critical buckling stress of steel tubes in both FRP-confined CFST columns and conventional CFST columns is proposed.

2. Local buckling modelling

2.1 General

Energy methods [30-33] are often employed to investigate the elastic local buckling behaviour of the steel plate in CFST columns, it is an effective method to study the local buckling behaviour of steel tubes in contact with concrete or rigid media as demonstrated by Wright [31-32], Long et al. [33-35] and Bradford et al. [36]. Furthermore, under arbitrary conditions of loading, energy methods have been shown to be more advantageous than the finite element method or the finite strip method [36]. Hence, energy methods are presently used to construct a model for local buckling of the steel tube in FRP-confined CFST columns, assuming that: (1) the steel tube is subjected to uniform compression; (2) the infilled concrete is regarded as a rigid medium; (3) the steel tube is free from initial geometric imperfections and residual stresses; (4) the buckling of the steel tube in the longitudinal direction includes a number of geometrically-compatible harmonics; and (5) the slip between the steel tube and the FRP jackets is neglected and the two components work as an integrated member before the steel tube buckles. These assumptions correspond with normal strategies for local buckling model of CFST columns [5,6,31-37] and most of these assumptions correspond with the experimental results of FRP-confined CFST columns [21-24].

2.2 Potential energy formulation

The local buckling mode of the steel tube in FRP-confined CFST columns is depicted in Fig. 2; as shown, the steel tube in FRP-confined CFST columns only buckles outwards due to the steel tube being restrained against buckling inwards by the infilled concrete. The steel tube is only subjected to a uniform compression N_x in the x direction, which is the uniform compression per unit length around the circumference of the steel tube.

Based on previous research on the local buckling of CFST columns [36], the local buckling displacement w can be described by the function w, thus:

$$w = -f \sin^2 \frac{m\pi x}{L} \tag{1}$$

where f is a generalized coordinate defining the amplitude of w and $f > 0$; L is the length of the steel tube; m is the number of buckling half wavelengths in the longitudinal (x) direction.

It is assumed that both ends of the steel tube are clamped, resulting in the conditions at x=0 and x=L being:

$$w=0 \tag{2}$$

$$\frac{\partial w}{\partial x}=0 \tag{3}$$

where the assumed expression for *w* automatically satisfies these boundary conditions.

The strain energy U_b of the steel tube from bending can be given by the standard expression [30]:

$$U_b=\frac{D_r}{2}\iint\left\{\left(\frac{\partial^2 w}{\partial x^2}+\frac{\partial^2 w}{\partial y^2}\right)^2-2\left(1-\mu_s\right)\left[\frac{\partial^2 w}{\partial x^2}\frac{\partial^2 w}{\partial y^2}-\left(\frac{\partial^2 w}{\partial x\partial y}\right)^2\right]\right\}dxdy \tag{4}$$

where D_r is the flexural rigidity of the steel tube, thus:

$$D_r=\frac{E_s t_s^{\ 3}}{12(1-\mu_s^{\ 2})} \tag{5}$$

in which t_s is the wall thickness of the steel tube; E_s and μ_s respectively are the Young's modulus and Poisson's ratio of the steel tube. The axisymmetric nature of the problem results in the function for *w* being in *x* only, hence:

$$\frac{\partial^2 w}{\partial y^2}=\frac{\partial^2 w}{\partial x\partial y}=0 \tag{6}$$

and so Eq. (4) automatically reduces to the following:

$$U_b=\frac{D_r}{2}\iint\left(\frac{\partial^2 w}{\partial x^2}\right)^2 dxdy \tag{7}$$

hence, substituting Eq. (1) into Eq. (7) gives

$$U_b=2D_r\left(\frac{m\pi}{L}\right)^4 f^2\pi rL \tag{8}$$

where *r* is the radius of the thin-walled steel tube such that $t_s/r<<1$.

Also, the strain energy of the steel tube arising from membrane stretching U_m can be expressed thus [30]:

$$U_m=\frac{E_s t_s}{2(1-\mu_s^{\ 2})}\iint\left[\left(\varepsilon_{x,s}+\varepsilon_{y,s}\right)^2-2\left(1-\mu_s\right)\left(\varepsilon_{x,s}\varepsilon_{y,s}-\frac{1}{4}\gamma_{xy,s}^2\right)\right]dxdy \tag{9}$$

in which $\varepsilon_{x,s}$, $\varepsilon_{y,s}$ and $\gamma_{xy,s}$ respectively are the longitudinal strain, the hoop strain and the shear strain within the steel tube. The axisymmetric nature of the problem results in the shear strain being zero, hence:

$$\gamma_{xy,s}=0 \tag{10}$$

and based on previous research on local buckling of CFST columns [37], the longitudinal strains and the hoop strains of the steel tube are given by

$$\varepsilon_{x,s}=\mu_s\frac{w}{r} \tag{11}$$

$$\varepsilon_{y,s}=-\frac{w}{r} \tag{12}$$

Substituting Eqs. (10), (11) and (12) into Eq. (9) gives

$$U_m=\frac{3}{8}\frac{E_s t_s}{r^2}f^2\pi rL \tag{13}$$

The work done W by the compressive force N_x is given by the standard expression [30]:

$$\begin{aligned}W&=\frac{1}{2}\iint N_x\left(\frac{\partial w}{\partial x}\right)^2dxdy\\&=\frac{1}{2}\iint-\sigma_x t_s\left(\frac{\partial w}{\partial x}\right)^2dxdy\\&=-\frac{1}{2}\left(\frac{m\pi}{L}\right)^2f^2\pi rL\sigma_x t_s\end{aligned} \tag{14}$$

Based on equilibrium, illustrated in Fig.3, the confining pressure on the steel tube provided by FRP jackets $\sigma_{r,s}$ is given by the expression:

$$\sigma_{r,s}=-\sigma_{r,frp}=\frac{E_{frp}\varepsilon_{y,frp}t_{frp}}{r} \tag{15}$$

It is assumed that the slip between the steel tube and the FRP jackets is neglected and the two components work as an integral component before the steel tube buckles, as detailed in Section 2.1, which results in:

$$\varepsilon_{y,frp}=\varepsilon_{y,s}=-\frac{w}{r} \tag{16}$$

Substituting Eq. (16) into Eq. (15) results in

$$\sigma_{r,s}=-\frac{E_{frp}t_{frp}w}{r^2} \tag{17}$$

Based on previous experimental studies on FRP-confined CFST columns [21-24], the properties of different types of FRP obtained from tests are listed in Table 1. Four types of fibre reinforced polymer (FRP) usually used in FRP-confined CFST columns are listed in Table 1 and respectively they are glass FRP (GFRP), aramid FRP (AFRP), carbon FRP (CFRP) and high modulus carbon FRP (HMFRP). As listed in Table 1, the hoop rupture strains of these FRP materials are much larger than the yield strain of the steel tube (i.e. $\varepsilon_{rup,frp} \geqslant 0.002$), resulting in the FRP jacket not rupturing before the occurrence of elastic local buckling of the steel tube, which corresponds with the assumptions in Section 2.1. Hence, the work done by the confining pressure $\sigma_{r,s}$ on the steel tube V, which is provided by FRP jackets, is given by

$$V = -\frac{1}{2}\iint \sigma_{r,s} w dxdy \tag{18}$$

Substituting Eq. (17) into Eq. (18) gives

$$V = \frac{3}{8}\frac{E_{frp}t_{frp}}{r^2} f^2 \pi r L \tag{19}$$

The total potential energy Π of the steel tube is thus:

$$\Pi = U_b + U_m + V + W \tag{20}$$

Substituting Eqs. (8), (13), (14) and (19) into Eq. (20) results in the following expression

$$\Pi = 2D_r\left(\frac{m\pi}{L}\right)^4 f^2\pi r L + \frac{3}{8}\frac{E_s t_s}{r^2} f^2 \pi r L + \frac{3}{8}\frac{E_{frp}t_{frp}}{r^2} f^2\pi r L - \frac{1}{2}\left(\frac{m\pi}{L}\right)^2 f^2 \pi r L \sigma_x t_s \tag{21}$$

The critical buckling stress of the steel tube can be determined by minimizing the total potential energy Π with respect to the generalized coordinate f, using the critical equilibrium condition $\frac{\partial^2 \Pi}{\partial f^2} = 0$. Solving the resulting equation gives the buckling stress σ_x

$$\sigma_x = \frac{4D_r}{t_s}\left(\frac{m\pi}{L}\right)^2 + \frac{3E_{frp}t_{frp} + 3E_s t_s}{4r^2 t_s}\left(\frac{m\pi}{L}\right)^{-2} \tag{22}$$

Minimizing σ_x with respect to the wave number m thus

$$\frac{\partial \sigma_{\mathrm{x}}}{\partial m} = 0 \tag{23}$$

results in the following relationship:

$$\frac{m\pi}{L} = \left(\frac{3E_{frp}t_{frp} + 3E_s t_s}{16 D_r r^2} \right)^{1/4} \tag{24}$$

Substituting Eq. (24) into Eq. (22) gives the local critical buckling stress σ_{cr} of the steel tube in FRP-confined CFST columns, which can be expressed thus:

$$\sigma_{cr} = \frac{2E_s}{\sqrt{1-\mu_s^2}} \frac{1}{d/t_s} \sqrt{1 + \frac{E_{frp}t_{frp}}{E_s t_s}} \tag{25}$$

Furthermore, Eq.(25) can be rewritten as

$$\sigma_{cr} = \frac{2E_s}{\sqrt{1-\mu_s^2}} \frac{1}{d/t_s} \left(1 + \frac{1}{1+\sqrt{1+\frac{E_{frp}t_{frp}}{E_s t_s}}} \frac{E_{frp}t_{frp}}{E_s t_s} \right) = \frac{2E_s}{\sqrt{1-\mu_s^2}} \frac{1}{d/t_s} (1+\beta) \tag{26}$$

where an influence coefficient β for the FRP jacket is proposed to evaluate its influence on the critical stress that is defined thus:

$$\beta = \frac{\alpha}{1+\sqrt{1+\alpha}} \tag{27}$$

in which α is the tensile stiffness ratio of FRP jackets to the steel tube that is given by

$$\alpha = \frac{E_{frp}t_{frp}}{E_s t_s} \tag{28}$$

Hence, substituting Eq. (27) into Eq. (26) gives a more compact expression of the local critical buckling stress σ_{cr}

$$\sigma_{cr} = \frac{2E_s}{\sqrt{1-\mu_{\mathrm{s}}^2}} \frac{1}{d/t_s} \left(1 + \frac{\alpha}{1+\sqrt{1+\alpha}} \right) \tag{29}$$

2.3 Calibration of the proposed model

Finite element models using the FE package ABAQUS [38] were developed to verify the proposed theoretical model. In accordance with the assumptions of the proposed theoretical model, global initial geometric imperfections and residual stresses were not included in FE models. The reference stub FRP-confined CFST columns with column length L=4500 mm, diameter of steel tube d=1500 mm (i.e. L/d =3) were adopted due to that the slenderness ratio (i.e. L/d ratio) does not influence the local buckling behaviour of the column when L/d ratio greater than or equal to 3.0. A suitable size of the uniform mesh was found to be 100mm×100 mm by performing a mesh convergence study.

The FE model includes three components: FRP, steel tube and concrete. Four-noded, reduced integration shell elements with six degrees of freedom per node, designated as S4R in the ABAQUS element library, were chosen for both the FRP Jacket and the steel tube in numerical models due to the successful employment in the previous simulations of FRP confined CFST columns or CFST columns [39-42]. Solid elements C3D8R were adopted for the core concrete [39-41]. Based on the assumption of the proposed theoretical model (see Section 2.1), there is no relative slip between the FRP and steel tube and the two components work as an integrated member before the steel tube buckles. Hence, a "Tie" constraint was adopted between the FRP and steel tube. In accordance with the assumptions of the proposed model, the concrete was designated as a rigid body in the numerical models. Moreover, the "hard contact" setting was used to define the normal contact surface between the contact surfaces of the steel tube and the concrete. The elastic material properties of structural steel (E_s= 206000 MPa and μ_s =0.3) and the elastic material properties FRP jackets were employed for all models. For simplicity, the material behaviour of the steel tube and FRP was assumed to be homogeneous, isotropic and linear elastic. Furthermore, the rupture strain of FRP was assumed to be extremely large so that FRP never ruptures during the loading, which corresponds with the proposed model.

Boundary conditions were applied to simulate fixed ends of the columns, which corresponds with the proposed theoretical model. This was achieved by restraining all the displacements and rotations at the base of the columns. The axial compressive load was applied at the centroid of the other rigid end plate, on which all the degrees-of-freedom except the longitudinal displacement were fixed. A linear eigenvalue analysis was performed, from which the elastic buckling stress for each buckling mode was obtained, including the elastic critical buckling stress associated with the first valid buckling mode.

The comparison of calculated local critical buckling stresses (σ_{cr}) of the steel tube in FRP-confined CFST columns in the cases of α=0.10 and α=0.25 between the proposed theoretical model and FE method is indicated in Fig.4, resulting in good agreement, which confirms that the proposed model is correct and consistent.

In addition, based on previous studies on FRP-confined CFST columns by Xiao et al. [18-21], Tao et al. [22] and

Teng et al. [23-24], the elastic local buckling of steel tubes in FRP-confined CFST columns does not occur due to FRP jackets. The proposed model is also verified against the test results of FRP-confined CFST columns from [21-24]. As listed in Table 2, the calculated local critical buckling stresses (σ_{cr}) from the proposed model are much greater than the yield strength of the steel tube (f_{sy}), indicating the steel tube would yield before any local buckling. Furthermore, experimental results from Refs. [21-24] showed the elastic local buckling did not occur for these specimens from Refs. [21-24] due to the confinement effects of FRP jackets on the steel tube, which corresponds with the calculated results of the proposed model.

In particular, when t_{frp}=0, i.e. the case of CFST columns without FRP jackets, Eq.(25) reduces to the following relationship:

$$\sigma_{cr} = \frac{2E_s}{\sqrt{1-\mu_s^2}} \frac{1}{d/t_s} \tag{30}$$

which corresponds to the results of the previous study on the local buckling behavior of CFST columns [36]. This indicates that the proposed model for local buckling of the steel tube in FRP-confined CFST columns is compatible with the previous models for CFST columns. Hence, the proposed model is appropriate for both FRP-confined CFST columns and conventional CFST columns.

3. Discussion

3.1 Influence of the tensile stiffness ratios

Based on the proposed model, i.e. Eq. (29), the influence of the tensile stiffness ratios of the FRP jackets to the steel tubes (α), and the diameter-to-thickness ratio of the steel tubes (d/t_s) on the local critical buckling stress (σ_{cr}) of the steel tube in FRP-confined CFST columns is indicated in Fig. 5. It is observed that the critical buckling stress (σ_{cr}) is significantly influenced by both the aforementioned ratios; the critical buckling stress σ_{cr} decreases with the increase of d/t_s, while σ_{cr} increases with increasing α at a specified value of the d/t_s ratio. Furthermore, based on the proposed model, i.e. Eqs.(26) and (29), the influence of the FRP jackets on σ_{cr} is only determined by the parameter α rather than d/t_s ratios.

3.2 Influence of FRP types and thickness ratios

Based on the proposed model, the influence of the FRP types and the thickness ratios of FRP jackets to the steel tube (i.e. $\gamma=t_{frp}/t_s$) on the local critical buckling stress (σ_{cr}) of the steel tube in FRP-confined CFST columns respectively are indicated in Figs. 6 and 7. Four types of FRP, which include glass FRP (GFRP), aramid FRP (AFRP), carbon FRP (CFRP) and high modulus CFRP (HMCFRP) that are detailed in Table 1, are employed to investigate the influence of the FRP types on σ_{cr}. As indicated in Fig. 6, the influence of the FRP types on σ_{cr} is determined by the elastic modulus of FRP jackets for the same thickness ratios of FRP jackets to the steel tube γ. For instance, the influence of GFRP and AFRP on σ_{cr} are almost the same due to their similar elastic moduli. The local critical buckling stress (σ_{cr}) of the steel tube in HMCFRP-confined CFST columns is the largest resulting from the highest elastic modulus. Furthermore, the influence of FRP types on σ_{cr} becomes significant with γ increasing (see Fig. 6). In addition, it may be observed from Fig. 7 that σ_{cr} increases with increasing γ for a specified FRP-confined CFST column. Generally, based on the proposed model (i.e. Eqs (26), (28) and (29)), it can be found that different FRP types (i.e. different the elastic modulus of FRP jackets) and different thickness ratios of FRP jackets to the steel tube γ usually lead to different the tensile stiffness ratios of the FRP jackets to the steel tubes (α), which eventually influence the local critical buckling stress (σ_{cr}) of the steel tube in FRP-confined CFST columns.

3.3 Reasonable limitations for diameter-to-thickness ratios

The yield strength f_{sy} of a mild structural steel tube usually employed for CFST columns is not greater than 450 MPa [33-35]; hence, $\sigma_{cr}\geq f_{sy}$=450MPa can ensure that the steel tube in FRP-confined CFST columns yields before elastic local buckling occurs. Then, substituting σ_{cr}=450MPa into Eq.(29) results in the reasonable ranges for the diameter-to-thickness ratios of the steel tube (d/t_s) in FRP-confined CFST columns, listed in Table 3. It can be found in Table 3 that the upper limit of d/t_s increases modestly with the increase of the thickness ratios of FRP jackets to the steel tube γ. It should be noted that the limits in Table 3 should be taken in account of the safety factors in engineering practice or serving as practical design guidelines.

3.4 Equivalent steel tube thickness

To achieve better understanding of the influence of the FRP jackets on the local critical buckling behavior of FRP-confined CFST columns, a novel concept that introduces an equivalent thickness t_{eq} of the steel tube contributed by the FRP jackets is proposed and thus:

$$t_{eq}=(1+\beta)t_s=\left(1+\frac{\alpha}{1+\sqrt{1+\alpha}}\right)t_s \tag{31}$$

in which β is the influence coefficient of the FRP jacket and α is the tensile stiffness ratio of the FRP jackets to the steel tube, as detailed in Eq.(27) and Eq.(28), respectively. From Eq.(30), the influence of FRP jackets on the critical buckling stress (i.e. βt_s) is included in the equivalent thickness of the steel tube in FRP-confined CFST columns based on the equivalence of the critical buckling stress. Hence, the local critical buckling stress σ_{cr} of the steel tube in FRP-confined CFST columns can be expressed in a new form i.e. within a unified equation of the local critical buckling stress of the steel tube in the form of an equivalent thickness of the steel tube contributed by the FRP jackets:

$$\sigma_{cr} = \frac{2E_s}{\sqrt{1-\mu_s^2}} \frac{1}{d/t_{eq}} \tag{32}$$

Additionally, it should be stressed that Eq. (32) is appropriate for both FRP-confined CFST columns and conventional CFST columns. When β=0 i.e. t_{eq}=t_s, Eq.(32) reduces to Eq.(30), reducing to the case of CFST columns without FRP jackets. Furthermore ,this concept i.e. Eq.(31) can be also extended to nonlinear or post-buckling regimes of the steel tube when FRP does not rupture, which may result in a relatively conservative result. Hence, the concept of equivalent steel tube thickness is still appropriate for post-buckling regimes of the steel tube. In essence, the equivalent steel tube thickness t_{eq} can reflect the contribution of FRP jackets to the local critical buckling stress of the composite column and result in that the local critical buckling stress can be expressed in a new form i.e Eq. (32).

7. Conclusions and remarks

An energy-based model for the local buckling of FRP-confined CFST columns is proposed, in which the influence of FRP jackets on the local buckling behavior of the steel tube is reasonably estimated. The proposed model is then calibrated against the results of an FE model and tests, indicating that the proposed model is correct and compatible with the previous model for conventional CFST columns. The proposed model is then employed to investigate the local buckling behavior of the steel tube in FRP-confined CFST columns under axial compression. It is found that the local critical buckling stress (σ_{cr}) of the steel tube in FRP-confined CFST columns is significantly influenced by both the tensile stiffness ratios of FRP jackets to the steel tube (α) and the diameter-to-thickness ratios of the steel tube (d/t_s). The local critical buckling stress (σ_{cr}) decreases with the diameter-to-thickness ratios of the steel tube increasing, it also increases with the tensile stiffness ratios of FRP jackets to the steel tube (α) increasing at a specified value of d/t_s ratio. The influence of FRP jackets on σ_{cr} is only determined by the parameter α instead of d/t_s ratios. Furthermore, limits for the diameter-to-thickness ratios of the steel tube in FRP-confined CFST columns are suggested for structural engineering practice.

In addition, a novel concept regarding an equivalent thickness t_{eq} of the steel tube contributed by the FRP jackets is proposed. The influence of the thickness of FRP jackets on the critical buckling stress σ_{cr} may be considered to be equivalent to that of an additional thickness of the steel tube (i.e. βt_s) based on the equivalence of σ_{cr}, resulting in a unified equation of the local critical buckling stress of the steel tube for both FRP-confined CFST columns and conventional CFST columns, which is readily usable in design practice.

Finally, it should be stressed the proposed model is appropriate for both FRP-confined CFST columns and conventional CFST columns, which bridges the gap between conventional CFST columns and FRP-confined CFST columns. The proposed model provides a better understanding of local buckling behaviour of FRP-confined CFST columns. Moreover, a unified method is also proposed to estimate the critical local buckling stress of FRP-confined CFST columns and conventional CFST columns for engineers, which can facilitate their practical design. The proposed model can be extended to nonlinear or post-buckling regimes of the steel tube when FRP does not rupture, which may result in a relatively conservative result. In addition, when debonding occurs between the FRP and steel tube or the FRP jackets rupture completely, the steel tube will not subject to the confinement of the FRP. The column will change from the FRP confined CFST column to the conventional CFST column. In this case, Eq.(25) and (29) for the model of FRP confined CFST columns will reduce to Eq.(30), which is suitable for conventional CFST columns. Particularly, when the FRP jackets partly rupture, the proposed model still works on the condition that the effective FRP jackets (excluding the ruptured FRP) can be quantified. Besides, the proposed model is not appropriate for the FRP-confined square CFST columns.

Acknowledgments

The authors would like to thank Miss Pui Yee Chung for her assistance. This research was funded by the National Natural Sciences Foundation of China (Grant No. 51008085 and Grant No. 11472084), Guangzhou Pearl River New Star of Science & Technology Project (Grant No. 2012J2200100), China Scholarship Council (Grant No. 201608440006) and China Postdoctoral Science Foundation (Grant No. 2012M511810 and No. 2014T70807).

References

[1] Furlong RW. Strength of steel-encased concrete beam-columns. J Struct. Div. ASCE 1967;93 (5):113-125.

[2] Furlong RW. Design of steel-encased concrete beam-columns. J Struct. Div. ASCE 1968;94 (1):267-281.

[3] Ge HB. Usami T. Strength of concrete-filled thin-walled steel box column: experiment. J Struct Eng ASCE 1992; 118 (11):3036-3054.

[4] Ge HB. Usami T. Strength analysis of concrete-filled thin-walled steel box column. J Constr Steel Res 1994; 30: 259-281.

[5] Uy B, Bradford MA. Elastic local buckling of steel plates in composite steel-concrete members. Eng Struct 1996; 18 (3):193-200.

[6] Bradford MA, Loh HY, Uy B. Slenderness limits for filled circular steel tubes. J Constr Steel Res 2002;58(3): 243-252.

[7] Sakino K., Nakahara H., Morino S., Nishiyama I. Behaviour of centrally loaded concrete-filled steel-tube short columns. J Struct Eng ASCE 2004;130 (2):180-188.

[8] Zuo Z.-L., Cai J, Yang C., Chen Q J. Eccentric load behavior of L-shaped CFT stub columns with binding bars. J Constr Steel Res 2012;72:105–118.

[9] Zuo Z.-L., Cai J, Yang C., Chen Q J. Sun G. Axial load behavior of L-shaped CFT stub columns with binding bars. Eng Struct 2012;37:88–98.

[10] Abed F, AlHamaydeh M, Abdalla S. Experimental and numerical investigations of the compressive behavior of concrete filled steel tubes (CFSTs). J Constr Steel Res 2013;80:429-439.

[11] Abdalla S, Abed F, AlHamaydeh M. Behavior of CFSTs and CCFSTs under quasi-static axial compression. J Constr Steel Res 2013; 90:235-244.

[12] Lai MH, Ho JCM. A theoretical axial stress-strain model for circular concrete-filled-steel-tube columns, Eng Struct 2016;125:124-143.

[13] Long Y.-L., Cai J. Stress-strain relationship of concrete confined by rectangular steel tubes with binding bars. J Constr Steel Res 2013; 88:1–14.

[14] Wang YT, Wang, Cai J, Long Y.-L. Hysteretic behavior of square CFT columns with binding bars. J Constr Steel Res 2017;131:162–175.

[15] Yu T, Hu YM, Teng JG. Cyclic lateral response of FRP-confined circular concrete-filled steel tubular columns. J Constr Steel Res 2016;124:12-22.

[16] Teng JG, Hu YM, Yu T. Stress–strain model for concrete in FRP-confined steel tubular columns. Eng Struct 2013;49 (4):156-167.

[17] Yu T, Hu YM, Teng JG. FRP-confined circular concrete-filled steel tubular columns under cyclic axial compression. J Constr Steel Res 2014;94:33-48.

[18] Xiao Y. Applications of FRP composites in concrete columns, Adv Struct Eng 2004;7(4):335-343.

[19] Xiao Y, Shen YL. Impact behaviors of CFT and CFRP confined CFT stub columns. J Compos Constr ASCE 2012;16(6):662-670

[20] Choi KK, Xiao Y. Analytical model of circular CFRP confined concrete-filled steel tubular columns under axial compression. J Compos Constr ASCE 2010;14 (1):125-133.

[21] Xiao Y, He W, Choi K. Confined concrete-filled tubular columns. J Struct Eng ASCE 2005;131(3):488-497.

[22] Tao Z, Han LH,Zhuang JP. Axial loading behavior of CFRP strengthened concrete-filled steel tubular stub columns. Adv Struct Eng 2007;10(1):37-46.

[23] Teng JG, Hu YM. Theoretical model for FRP-confined circular concrete-filled steel tubes under axial compression. In: Proceedings, 3rd international conference on FRP composites in civil engineering, Miami, Florida, USA, 13–15 December, 2006. p. 503-506.

[24] Hu YM, Teng JG , Yu T. FRP-confined circular concrete-filled thin steel tubes under axial compression. J Compos Constr ASCE 2011;15(5):850-860.

[25] Prabhu GG, Sundarraja MC, Kim YY. Compressive behavior of circular CFST columns externally reinforced using CFRP composites. Thin-Walled Struct 2015;87:139-148.

[26] Sundarraja MC, Prabhu GG. Experimental study on CFST members strengthened by CFRP composites under compression. J Constr Steel Res 2012;72:75-83.

[27] Dong CX, Kwan AKH, Ho JCM. Axial and lateral stress-strain model for concrete-filled steel tubes with FRP jackets. Eng Struct 2016;126:365-378.

[28] Alam MI, Fawzia S, Zhao X-L, Remennikov AM, Bambach MR, Elchalakani M. Performance and dynamic behaviour of FRP strengthened CFST members subjected to lateral impact. Eng Struct 2017;147:160-176.

[29] Shen Q, Wang J, Wang J, Ding Z. Axial compressive performance of circular CFST columns partially wrapped by carbon FRP. J Constr Steel Res 2019;155:90-106.

[30] Timoshenko SP, Gere JM. Theory of Elastic Stability, 2nd ed., McGraw-Hill, NewYork, 1961.

[31] Wright HD. Buckling of steel plates in contact with a rigid medium. Struct Eng 1993;71(12):209–215.

[32] Wright H.D. Local stability of filled and encased steel sections. J Struct Eng ASCE 1995;121(10):1382–1388.

[33] Long Y.-L., Wan J, Cai J. Theoretical study on local buckling of rectangular CFT columns under eccentric compression. J Constr Steel Res2016;120:70-80.

[34] Long Y.-L., Zeng L. A refined model for local buckling of rectangular CFST columns with binding bars. Thin-Walled Struct 2018;132:431-441.

[35] Cai J, Long Y.-L. Local buckling of steel plates in rectangular CFT stub columns with binding bars. J Constr Steel Res 2009;65 (4):965–972.

[36] Bradford MA, Loh HY, Uy B. Slenderness limits for filled circular steel tubes. J Constr Steel Res 2002; 58:243–252.

[37] Jiang L, Zhou W, Liu P. Theoretical analysis of local buckling behavior about concrete filled steel tube column with axial compression. Journal of Building Structures 2011; 32(4):110-116 (in Chinese).

[38] ABAQUS. ABAQUS/Standard user’s manual volumes I–III and ABAQUS CAE manual. Version 6.4. (Pawtucket, USA): Hibbitt, Karlsson & Sorensen, Inc; 2004.

[39] Xu L, Hu H-S, Peng B, Guo Z-X. Seismic performance of composite jacket-confined square high-strength concrete-filled steel tube columns. J Constr Steel Res 2023;211:108128.

[40] Tan QH, Gardner L, Han LH, Song TY. Fire performance of steel reinforced concrete-filled stainless steel tubular (CFSST) columns with square cross-sections. Thin-Walled Structures 2019;143:106197.

[41] Wang F, Young B, Gardner L. CFDST sections with square stainless steel outer tubes under axial compression: Experimental investigation, numerical modelling and design. Eng Struct 2020;207:110189.

[42] Wang F, Young B, Gardner, L. Experimental study of square and rectangular CFDST sections with stainless steel outer tubes under axial compression. J Struct Eng ASCE 2019;145(11):04019139.

Nomenclature

d	diameter of steel tube
r	radius of steel tube
t_s	wall thickness of steel tube
t_{frp}	thickness of FRP jacket
L	length of steel tube
μ_s	Possion's ration of steel tube
m	number of half buckling wavelengths
f_{sy}	yield strength of steel tube
D_r	flexural rigidity of the steel tube
E_s	elastic modulus of steel tube
E_{frp}	elastic modulus of FRP jacket
N_x	surface force in the direction of x-axis
σ_x	normal stress acting on cross sections perpendicular to the x-axis and in the direction of the x-axis
$\sigma_{r,s}$	confining pressure on the steel tube provided by FRP jackets
$\varepsilon_{x,s}$	longitudinal strain of the steel tube
$\varepsilon_{y,s}$	hoop strain of the steel tube
$\gamma_{xy,s}$	shear strain of the steel tube
$\varepsilon_{y,frp}$	hoop strain of FRP jacket
$\varepsilon_{rup,frp}$	hoop rupture strain of FRP jacket
β	influence coefficient of FRP jackets on the critical stress of the steel tube
w	buckling displacement function
f	generalised coordinate defining amplitude of w
σ_{cr}	local critical buckling stress of the steel tube
γ	thickness ratio of FRP jackets to the steel tube
α	tensile stiffness ratio of FRP jackets to the steel tube
V	work done by the confining pressure on the steel tube provided by FRP jackets
W	work done by the compressive force
U_b	strain energy of the steel tube due to bending
U_m	strain energy of the steel tube due to membrane stretching
Π	total potential energy of the steel tube

Figures：Fig.1-Fig.7

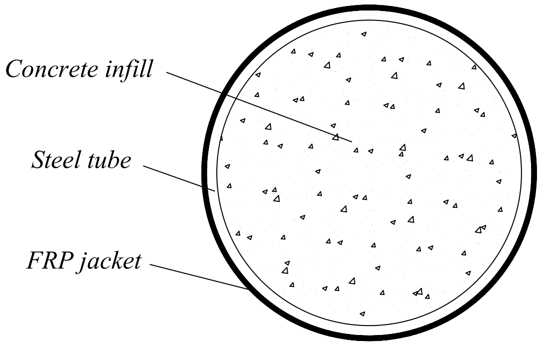

Fig. 1 Cross-section of FRP-confined CFST columns

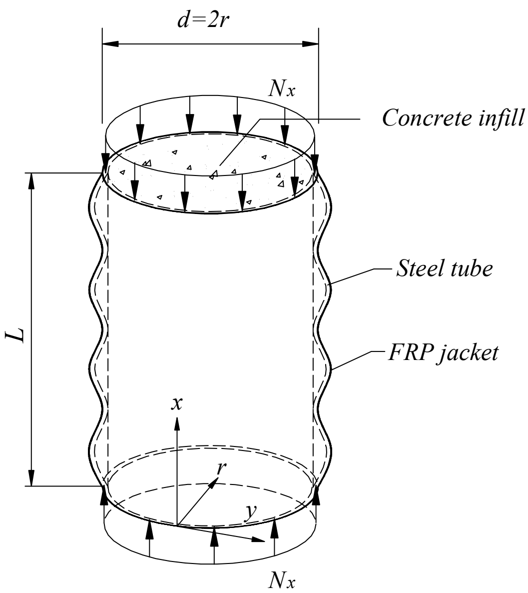

Fig. 2 Local buckling of the steel tube in FRP-confined CFST columns

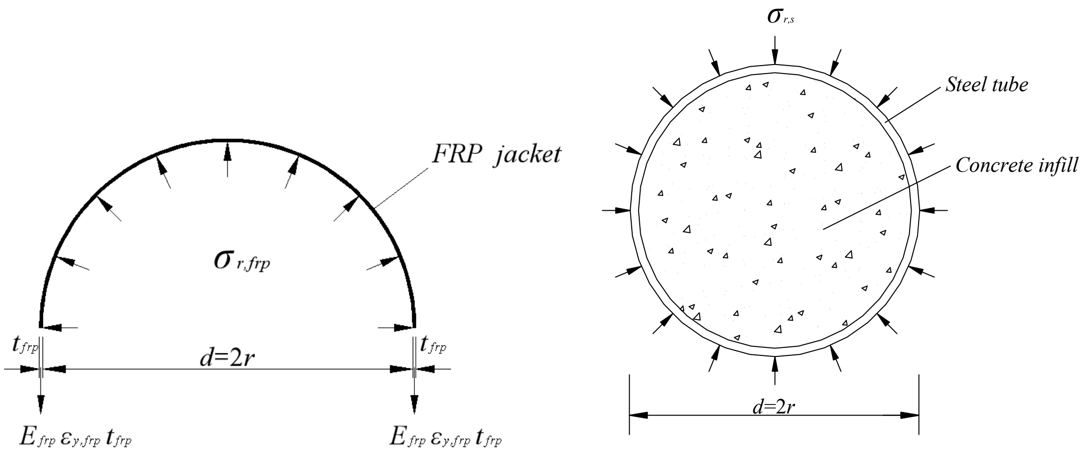

Fig. 3 Confining actions between the FRP jacket and the steel tube of FRP-confined CFST columns

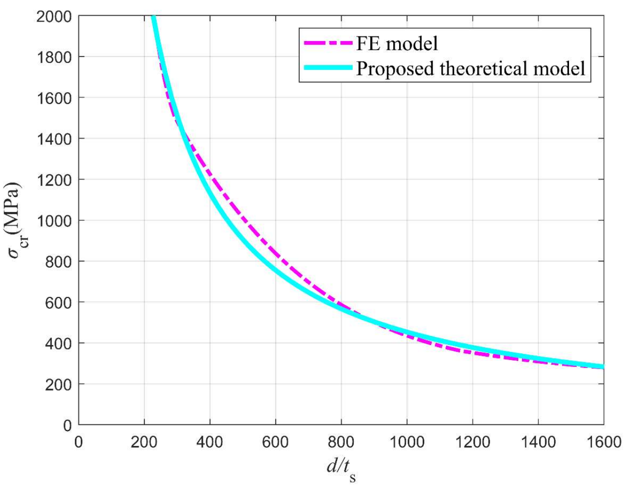

(a) α=0.10

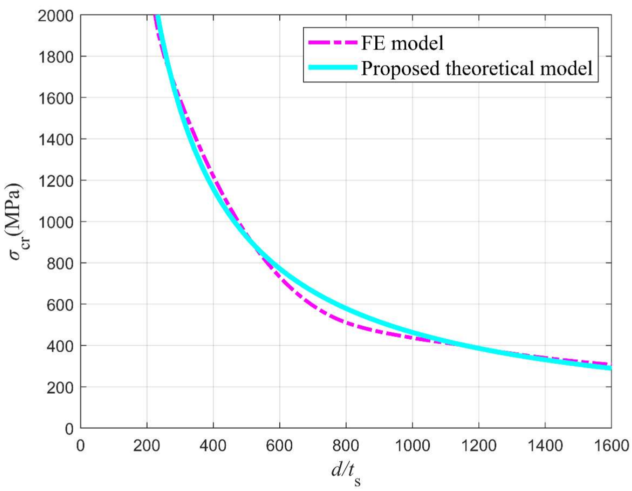

(b) α=0.15

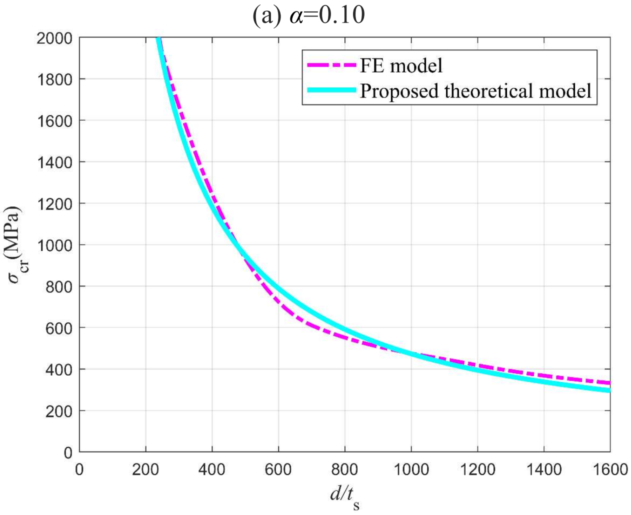

(c)α=0.20

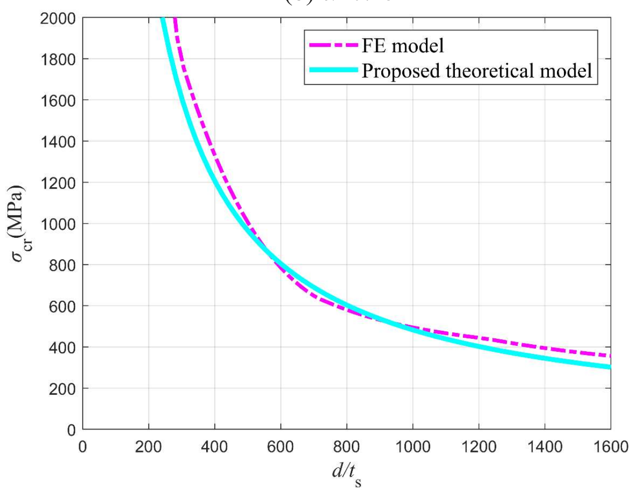

(d) α=0.25

Fig. 4 Comparison of elastic buckling stresses (σ_{cr}) calculated using the proposed model with those using the FE model

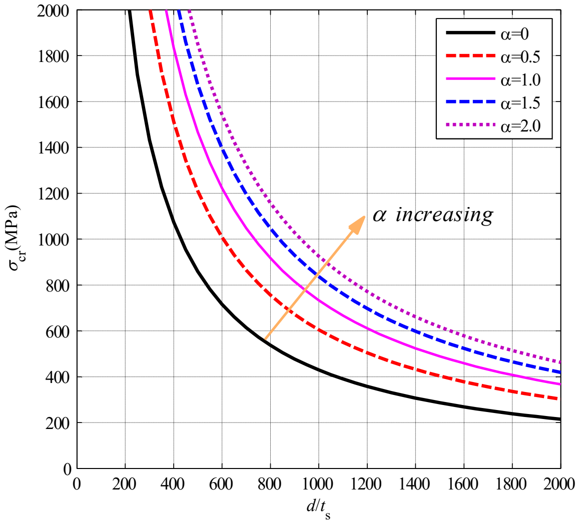

Fig. 5 Influence of α and d_s/t_s ratios on σ_{cr}

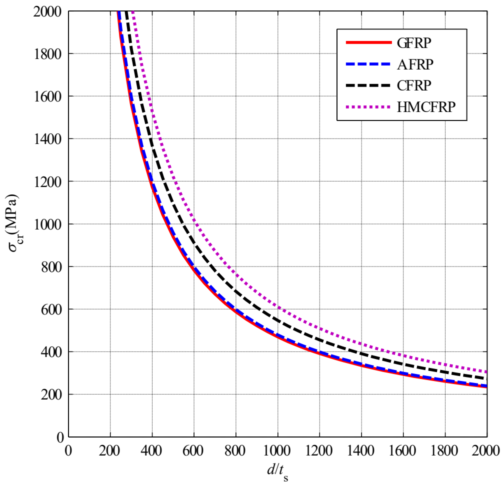

(a) γ=0.5

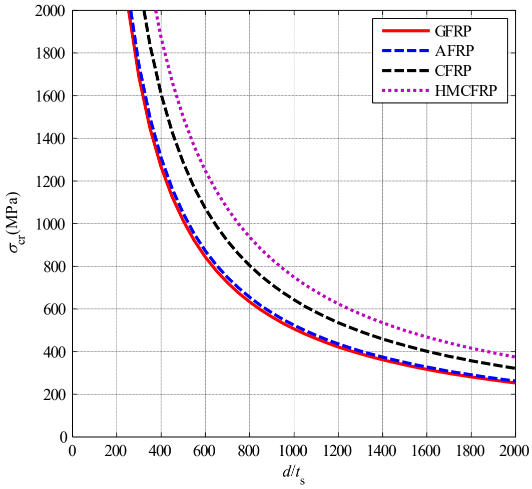

(b) γ=1.0

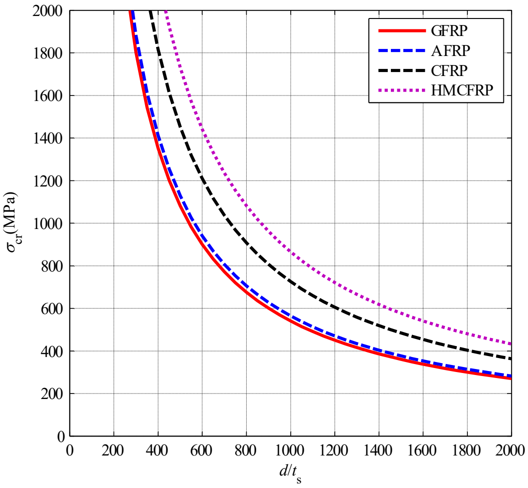

(c) γ=1.5

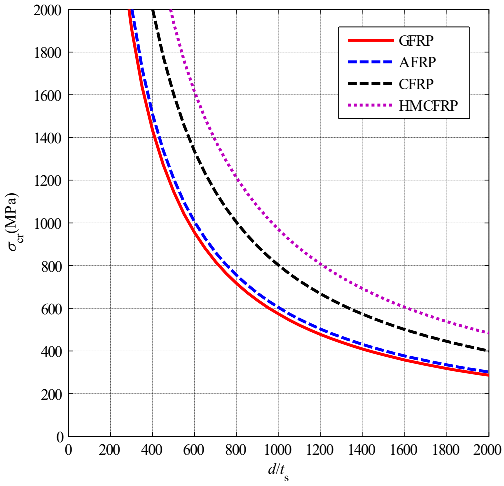

(d) γ=2.0

Fig. 6 Influence of FRP types on σ_{cr}

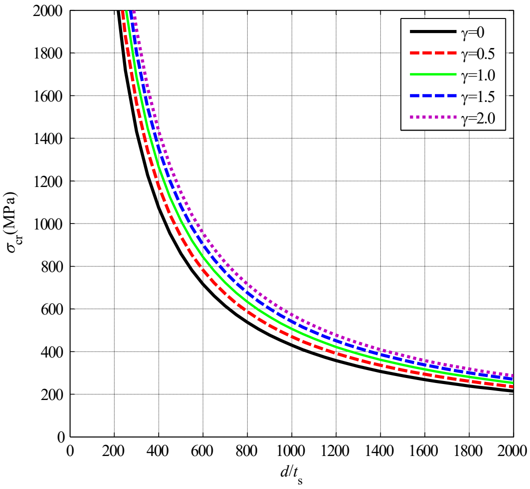

(a) GFRP-confined CFST columns

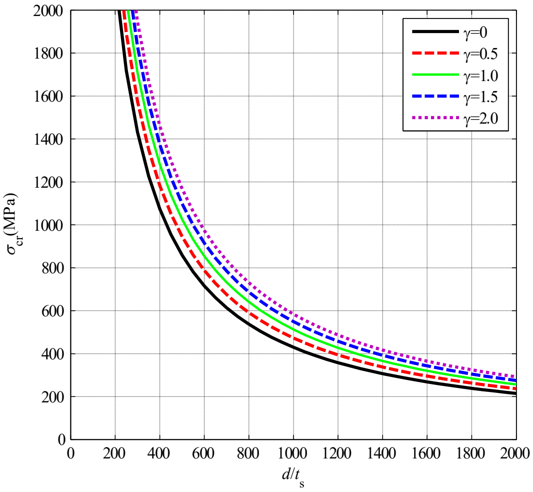

(b) AFRP-confined CFST columns

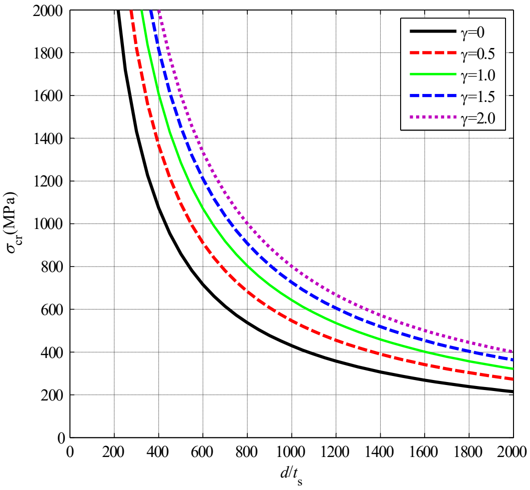

(c) CFRP-confined CFST columns

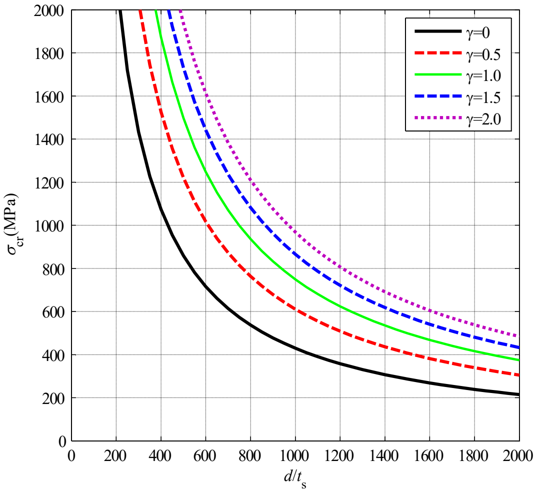

(d)HMCFRP-confined CFST columns

Fig. 7 Influence of γ on σ_{cr} for various typed FRP-confined CFST columns

Tables: Table1-Table3

Table 1. Properties of different types of FRP. Data sources: [21-24]

FRP type	E_{frp} (GPa)	$\varepsilon_{rup,frp}$
GFRP	80.1	0.0175
AFRP	87.3	0.0189
CFRP	255	0.0087
HMCFRP	420	0.0035

Table 2. Comparison of test results with those calculated by the proposed model for local buckling stress of steel tubes in FRP-confined CFST columns under axial compression

Specimen no.	d (mm)	t_s (mm)	d/t_s	E_s (GPa)	f_{sy} (MPa)	t_{frp} (mm)	E_{frp} (GPa)	f_{sy} (MPa)	α	σ_{cr} (MPa)	Ref.
CCFT-2L	152	2.95	51.5	206	356	2.8	64.9	356	0.30	10524	[21]
CCFT-4L	152	2.95	51.5	206	356	5.6	64.9	356	0.60	12281	
C1-0	156	3.0	52	206	230	0	255	230	0	8261	
C1-1	156	3.0	52	206	230	0.17	255	230	0.07	8821	
C1-2	156	3.0	52	206	230	0.34	255	230	0.14	9346	[22]
C2-0	250	3.0	83.3	206	230	0	255	230	0.00	5155	
C2-1	250	3.0	83.3	206	230	0.17	255	230	0.07	5504	
C2-2	250	3.0	83.3	206	230	0.34	255	230	0.14	5832	
F0-60	165	2.75	60	203	385.9	0	80.1	385.9	0.00	7055	
F1-60	165	2.75	60	203	385.9	0.17	80.1	385.9	0.02	7225	[23]
F2-60	165	2.75	60	203	385.9	0.34	80.1	385.9	0.05	7391	
F3-60	165	2.75	60	203	385.9	0.51	80.1	385.9	0.07	7553	
F0-102	204	2	102	203	226	0	80.1	226	0	4150	
F1-102	204	2	102	203	226	0.17	80.1	226	0.03	4287	
F2-102	204	2	102	203	226	0.34	80.1	226	0.07	4420	
F3-102	204	2	102	203	226	0.51	80.1	226	0.10	4548	
F0-135	203	1.5	135	204	242	0	80.1	242	0	3151	
F2-135	203	1.5	135	204	242	0.34	80.1	242	0.09	3420	
F3-135	203	1.5	135	204	242	0.51	80.1	242	0.13	3546	[24]
F4-135	203	1.5	135	204	242	0.68	80.1	242	0.18	3668	
F0-202	202	1	202	203	231	0	80.1	231	0	2096	
F2-202	202	1	202	203	231	0.34	80.1	231	0.13	2360	
F3-202	202	1	202	203	231	0.51	80.1	231	0.20	2480	
F4-202	202	1	202	203	231	0.68	80.1	231	0.27	2595	

Table 3. Suggested reasonable d/t_s ratios for steel tubes at different values of γ for various types of FRP-confined CFST columns under axial compression

γ	GFRP-confined CFST column	AFRP-confined CFST column	CFRP-confined CFST column	HMCFRP-confined CFST column
0.2	$d/t_s \le 992$	$d/t_s \le 995$	$d/t_s \le 1067$	$d/t_s \le 1134$
0.4	$d/t_s \le 1027$	$d/t_s \le 1033$	$d/t_s \le 1169$	$d/t_s \le 1288$
0.6	$d/t_s \le 1061$	$d/t_s \le 1070$	$d/t_s \le 1262$	$d/t_s \le 1426$
0.8	$d/t_s \le 1094$	$d/t_s \le 1106$	$d/t_s \le 1349$	$d/t_s \le 1552$
1.0	$d/t_s \le 1126$	$d/t_s \le 1140$	$d/t_s \le 1431$	$d/t_s \le 1668$
1.2	$d/t_s \le 1158$	$d/t_s \le 1174$	$d/t_s \le 1508$	$d/t_s \le 1776$
1.4	$d/t_s \le 1188$	$d/t_s \le 1207$	$d/t_s \le 1581$	$d/t_s \le 1878$
1.6	$d/t_s \le 1218$	$d/t_s \le 1238$	$d/t_s \le 1652$	$d/t_s \le 1975$
1.8	$d/t_s \le 1247$	$d/t_s \le 1269$	$d/t_s \le 1719$	$d/t_s \le 2068$
2.0	$d/t_s \le 1275$	$d/t_s \le 1300$	$d/t_s \le 1784$	$d/t_s \le 2156$